JOC The Journal of Organic Chemistry

Article

pubs.acs.org/joc

Synthesis, Reactivity, and Spectroscopic Properties of *meso*-Triaryl-5-oxaporphyrins

Kazuhisa Kakeya, Aya Nakagawa, Tadashi Mizutani,* Yutaka Hitomi, and Masahito Kodera

Department of Molecular Chemistry and Biochemistry, Faculty of Science and Engineering, and Center for Nanoscience Research, Doshisha University, Kyotanabe, Kyoto 610-0321, Japan

Supporting Information

ABSTRACT: [*meso*-Triaryl-21,23-didehydro-23*H*-5-oxaporphyrinato](trifluoroacetato)zinc(II) was prepared by the reaction of *meso*-triarylbilindione with acetic anhydride and zinc acetate, and it was isolated as a trifluoroacetate salt. The X-ray crystallographic study demonstrated that the trifluoroacetate anion was coordinated to the zinc ion. [21,23-Didehydro-10,15,20-tris(4-methoxycarbonylphenyl)-23*H*-5-oxaporphyrinato](trifluoroacetato)zinc(II) **3a** was dissolved in various organic solvents such as toluene, chloroform, diethyl ether, ethyl acetate, acetone, acetonitrile, methanol, DMSO, and DMF, although it readily reacted with alcohols and DMF to yield linear tetrapyrroles. The solubility of **3a** in toluene was 4.2 ± 0.1 g dm^{-3} at room temperature. **3a** showed characteristic UV−vis absorption at 649 nm and fluorescence emission at 657 nm in chloroform. The fluorescence quantum yields of **3a**, [21,23-didehydro-10,15,20-triphenyl-23*H*-5-oxaporphyrinato](trifluoroacetato)zinc(II) (**3c**), and [21,23-didehydro-10,15,20-tris(4-methoxyphenyl)-23*H*-5-oxaporphyrinato](trifluoroacetato)zinc(II) (**3b**) were 0.071, 0.071, and 0.050, respectively. Reaction of **3a** with EtOH afforded the zinc complex of 19-ethoxybilinone, and it proceeded 2 orders of magnitude faster than that of [*β*-octaalkyl-21,23-didehydro-23*H*-5-oxaporphyrinato]zinc(II). The reaction with alcohols was sensitive to steric bulk of the alcohols; the rate of reaction with *i*-PrOH was 2700 times faster than that of *t*-BuOH at 303 K. The reaction of [*meso*-triaryl-21,23-didehydro-23*H*-5-oxaporphyrinato]zinc(II) with water proceeded 3 orders of magnitude slower than that with EtOH.

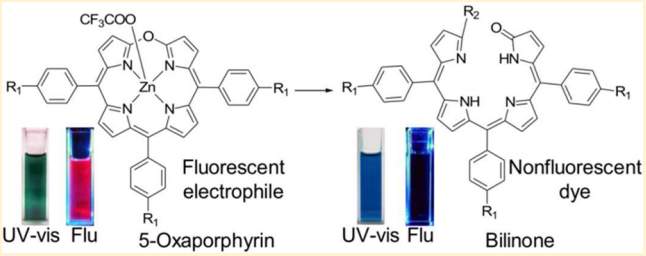

INTRODUCTION

Oxidation of iron porphyrin with O_2 is an important pathway of heme catabolism.[1] Several intermediates are shown to be involved such as 5-hydroxyporphyrin (oxophlorin) and 5-oxaporphyrin Fe complex (verdoheme). Thus, preparation of 5-oxaporphyrin and its spectroscopic properties and reactivity attract interest in decades. Jackson, Kenner, and Smith reported that oxidation of the iron complex of oxophlorin with O_2 in pyridine gave the oxaporphyrin iron complex.[2] Saito and Itano reported that the iron complex of *β*-octaethyl-5-oxaporphyrin was prepared from octaethylbilindione by the reaction with acetic anhydride, pyridine and iron sulfate.[3] Fuhrhop and co-workers described preparation of *β*-octaethyl-5-oxaporphyrin zinc complex from *β*-octaethylbilindione by the reaction with acetic anhydride or from octaethyloxophlorin by photochemical oxidation.[4] 5-Oxaporphyrin Fe(II) complexes were prepared by coupled oxidation reaction of porphyrin iron complexes with O_2 in the presence of ascorbic acid or hydrazine.[5] Preparation of cobalt[6] and copper[7] complexes of 5-oxaporphyrin by oxidation of porphyrins was also reported.

5-Oxaporphyrins are valuable precursors of linear tetrapyrroles because of the high reactivity toward nucleophiles. For instance, [5-oxaporphyrinato]zinc(II) was allowed to react with various nucleophiles such as alkoxide, Na_2S, or NH_3 to afford 19-alkoxybilinone, 5-thioniaporphyrin, and 5-azaporphyrin, respectively.[8−10] The reaction of 5-oxaporphyrin with diol or triol was used to prepare bilinone dimers and trimers.[11,12] The nucleophilic ring-opening of 5-oxaporphyrin complexes of Fe(II), Co(II), and Zn(II) was studied as a model reaction for verdoheme to biliverdin transformation.[13]

We previously reported that coupled oxidation of [*meso*-tetraarylporphyrinato]iron(III) yielded both biladienone and bilindione.[14] It is well-known that two porphyrins, *meso*-tetraphenylporphyrin and *β*-octaalkylporphyrin, have different reactivity,[15] since the electronic effects of alkyl groups are different from those of phenyl groups and the substitution pattern significantly affects the electronic structure of the porphyrin ring. *meso*-Tetraarylporphyrins have advantages over *β*-octaalkylporphyrins with respect to a simpler synthetic route and facile control of electronic structure by introducing various functional groups in the aryl groups. In addition, solubility of *meso*-tetraphenylporphyrin was higher than *β*-octaethylporphyrin in nonpolar solvents such as dichloromethane and toluene.[16] In addition to previously reported studies of 5-oxaporphyrins and bilindiones bearing *β*-octaalkyl substituents, investigations of *meso*-substituted analogues should extend the scope of tetrapyrrole chemistry, and such dyes should find applications

Received: May 23, 2012
Published: July 17, 2012

   dx.doi.org/10.1021/jo3010342 | J. Org. Chem. 2012, 77, 6510−6519

Scheme 1. Synthetic Route to [21,23-Didehydro-23*H*-5-oxaporphyrinato](trifluoroacetato)zinc(II) 3a–c[a]

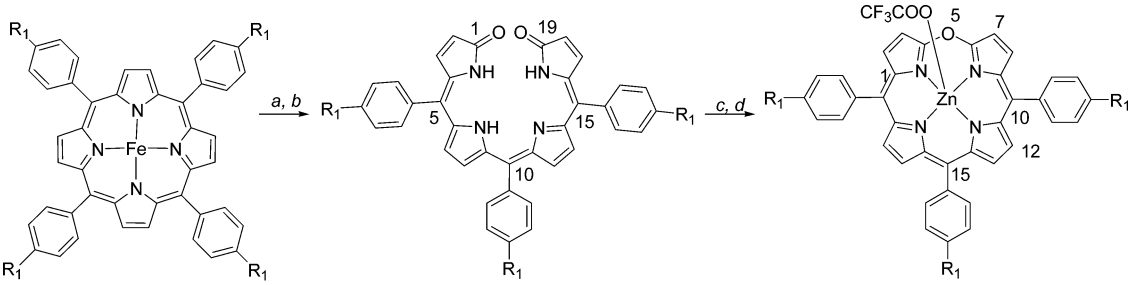

[a]Reagents: (a) O_2, ascorbic acid, pyridine in $CHCl_3$ at rt; (b) 2 M HCl; (c) Ac_2O, $Zn(OAc)_2$, ethanol-free $CHCl_3$, reflux; (d) 0.1%TFA.

in various fields. These tetrapyrrolic dyes find applications in electronic functional materials,[17] photofunctional materials,[18] and scaffolds of supramolecular architectures.[19] The goal of our study is to clarify structural, spectroscopic, and chemical properties of *meso*-triaryl derivatives of 5-oxaporphyrins and bilinones. In this paper, we report preparation of *meso*-triaryl-21,23-didehydro-23*H*-5-oxaporphyrins from bilindiones and investigations into the electrophilic reactivities and spectroscopic properties.

RESULTS AND DISCUSSION

Synthesis of 5-Oxaporphyrins. *meso*-Triarylbilindione **2** was prepared from [*meso*-tetraarylporphyrinato]iron(III) **1** by the coupled oxidation reaction (Scheme 1).[14a,c] The reaction of bilindione **2** with acetic anhydride and zinc acetate in ethanol-free chloroform under refluxing conditions for 1 h afforded the 5-oxaporphyrin zinc complex in a quantitative yield.[4b] Three [21,23-didehydro-23*H*-5-oxaporphyrinato]zinc(II) compounds **3a–c** having 4-methoxycarbonylphenyl, 4-methoxyphenyl, and phenyl groups on the meso positions were prepared. Chromatographic purification on SiO_2 using CH_2Cl_2/acetone/TFA (20/1/0.1) as eluent gave [21,23-didehydro-23*H*-5-oxaporphyrinato](trifluoroacetato)zinc(II) (**3**) as a green solid.

5-Oxaporphyrin **3a** was dissolved in various organic solvents such as toluene, chloroform, dichloromethane, diethyl ether, THF, ethyl acetate, acetone, acetonitrile, methanol, ethanol, DMSO, and DMF, although it was not stable in alcohols and DMF with spontaneous decomposition to yield linear tetrapyrroles. It is interesting to note that **3a** was slightly soluble even in water and hexane. The solubility of **3a** in toluene was 4.2 ± 0.1 g dm^{-3} at room temperature. Recently, Dechaine and co-workers reported that solubility of *β*-octaethylporphyrin and *meso*-tetraphenylporphyrin was 0.202 and 2.68 g dm^{-3} in toluene, respectively.[16] The solubility of **3a** in toluene was higher than *β*-octaethylporphyrin and *meso*-tetraphenylporphyrin.

The UV–vis spectra of **2a** and **3a** are shown in Figure 1. 5-Oxaporphyrin **3a** exhibited characteristic absorption peaks at 391 nm (B band) and 649 nm (Q-band). The spectrum is similar to [*β*-octaethyl-5-oxaporphyrinato]zinc(II) reported by Fuhrhop and co-workers, where the absorption maximum in chloroform was 662 nm.[4a] The molar absorption coefficient of the Q-band of 5-oxaporphyrin is ca. twice as large as that of Q_{0-1} of zinc *meso*-tetraphenylporphyrin.[20] There are two possible mechanisms for the intensified Q-band. First, the

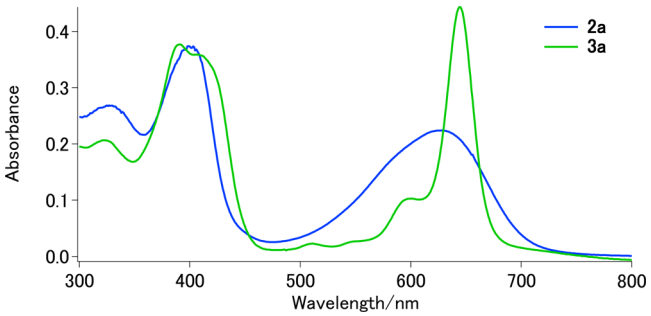

Figure 1. UV–vis spectra of **2a** and **3a** (1×10^{-5} M) in chloroform at 298 K.

degeneracy of the HOMO/LUMO of porphyrin is removed by replacement of the meso carbon with oxygen, since the molecular orbitals having large meso probabilities are stabilized.[21] Therefore, the Q-band is no longer a forbidden transition. Second, the transition electric dipole moment along the O5–C15 is intensified by the polarization due to the meso oxygen. We performed time-dependent HF/6-31G(d,p)//HF/6-31G(d,p) calculations of UV–vis spectra of **3a–c**, and transition energy, oscilator strength, and transition electric dipole moment directions are listed in Tables S7–S9 (see the Supporting Information). As shown in Tables S7–S9 (Supporting Information), the transition electric dipole moment direction of the Q-band is along the C10–C20 axis. Thus, the first mechanism, where the removed degeneracy of HOMO/LUMO caused the allowed Q-band, can account for the intense Q-band. Another characteristic feature of the UV–vis spectrum of 5-oxaporphyrin is the split B-band. As shown in Tables S7–S9 (Supporting Information), the split B-band is attributed to the perpendicularly polized two transitions, along the O5–C15 axis and the C10–C20 axis. Thus, removal of degeneracy of transitions along the C5–C15 axis and the C10–C20 axis resulted in the split B-band.

The TOF-mass spectrum of **3a** showed a peak at *m*/*z* 777 (M − CF_3COO^+) (M = $C_{45}H_{29}F_3N_4O_9Zn$). The ^1H NMR resonances of pyrrole *β*-protons of **3a** appeared at 7.76, 7.92, 8.09, and 8.22 ppm, while those of bilindione **2a** appeared at 6.26, 6.47, 6.69, and 6.94 ppm. The downfield shifts of these protons of **3a** by ca. 1.4 ppm as compared to **2a** demonstrated that these pyrrole *β*-protons have ring-current effects[8] due to the aromaticity of 5-oxaporphyrin. The ^1H NMR resonances of pyrrole *β*-protons of [5,10,15,20-tetrakis(4-methoxycarbonylphenyl)porphyrinato]zinc appeared at 8.8 ppm; thus,

dx.doi.org/10.1021/jo3010342 | J. Org. Chem. 2012, 77, 6510–6519

the aromaticity of **3a** was lower than the zinc porphyrin. The COSY experiments revealed that the resonances at 7.76 and 7.92 ppm are ascribed to the same pyrrole ring protons and those at 8.09 ppm and 8.22 ppm to the same pyrrole ring protons. The selected resonances in the ^{13}C NMR of **3a** appeared at 120.0, 130.6, 130.8, 134.5, 135.9, 140.7, 143.0, 150.0, 154.6, 165.4, 166.76, and 166.81 ppm. The peaks at 166.76 and 166.81 ppm were correlated with methyl ester protons at 4.04 and 4.06 ppm by the HMBC experiments; therefore, the peaks at 166.76 and 166.81 ppm were ascribed to the ester carbonyl carbons. Furthermore the HMBC experiments indicated that the resonances at 8.09 and 8.22 ppm show long-range coupling with the resonance at 165.4 ppm in the ^{13}C NMR. Because these 1D and 2D NMR experiments did not give conclusive evidence to differentiate the pyrroles bridged by oxygen and the other pyrroles, we also used the ^{1}H and ^{13}C NMR chemical shifts calculated with ab initio molecular orbital to assign the resonances. On the basis of ab initio calculations (HF/6-311+G(2d,p)) of NMR chemical shifts, the resonances at 8.09, 8.22, and 165.4 ppm were assigned to H3, H2, and C4, respectively. The resonance of C4 in the low magnetic field implies that the C4 carbon is electron deficient as is discussed below.

X-ray Crystallographic Studies of 3a. Crystals of **3a** were obtained by slow diffusion of cyclohexane to a solution of **3a** in toluene. The crystallographic studies revealed that the CF_3COO group was coordinated to the zinc, and the Zn−O distance was 2.010 (4) Å. An ORTEP view of the complex is shown in Figure 2. The 5-oxaporphyrin core was almost planar.

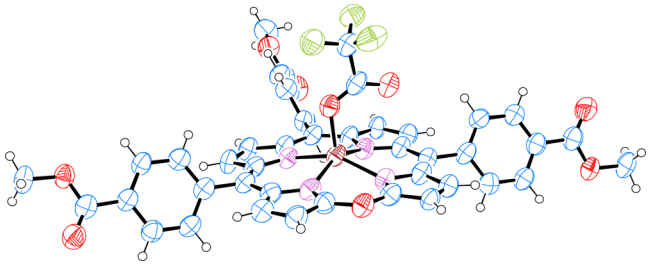

Figure 2. ORTEP view of **3a**.

The zinc ion is displaced 0.56 Å out of the 5-oxaporphyrin plane. The 5-oxaporphyrin plane is thus domed.[13] The displacements of each atom from the mean oxaporphyrin core plane are shown in Figure 3. The phenyl groups are tilted: the dihedral angles of C(pyrrole α)−C(meso)−C(phenyl ipso)−C(phenyl ortho) are 60 − 66°. The structure displays disorder in the location of the fluorine atoms of the ligand as well as solvent atoms (hexane). These were refined isotropically, while the remaining nonhydrogen atoms were refined anisotropically. The bond distances of **3a** are shown in Figure 4a and also listed in Table S2 (see the Supporting Information).

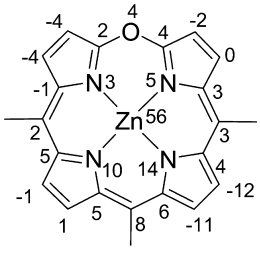

Figure 3. Perpendicular displacements of each atom of **3a** out of the mean oxaporphyrin core plane in units of pm.

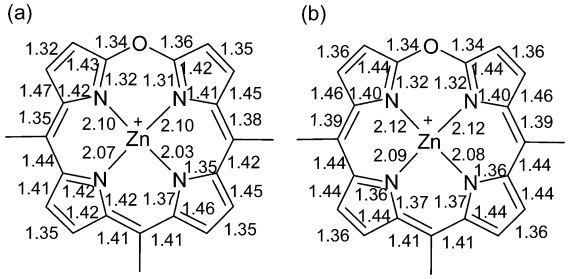

Figure 4. Bond distances (Å) of **3a**: (a) X-ray data and (b) ab initio calculations at B3LYP/6-31G(d).

The bond distances between the ring oxygen and the adjacent carbon atoms are 1.335(7) and 1.364(7) Å. This bond distances were a bit longer than carbonyl groups: a typical bond length of C═O in the carbonyl group is 1.23 Å.

Ab initio molecular orbital calculations were performed to gain further insights into the electronic structures of 5-oxaporphyrin. The bond orders computed by ab initio molecular orbital (B3LYP/6-31G(d)//B3LYP/6-31G(d)) are shown in Figure S16 (Supporting Information). The bond order between the ring oxygen and the adjacent carbon atoms was 1.02. The bond orders between the ring oxygen and the adjacent carbon in furan computed by the AM1 semiempirical method[22] and the Møller−Plesset (MP2) method[23] were 1.10 and 0.98, respectively. In addition, the bond distance of furan was studied by microwave[24] and electron diffraction.[25] According to the microwave experiment, the C−O bond distance in furan is 1.36 Å. Comparisons of the bond distances and bond orders between furan and 5-oxaporphyrin indicate that the C−O bond in the macrocycle of 5-oxaporphyrin is similar to that of furan.

For the bond order of the meso carbon to pyrrole α carbon, the bond distance of C9−C10 was 1.379(7) Å and significantly shorter than that of C10−C11 (1.422(7) Å). Therefore, the C9−C10 bond had a larger bond order than the C10−C11 bond. Bond distances calculated using ab initio molecular orbital theory at the B3LYP/6-31G(d) level for geometry optimization are shown in Figure 4b. Figure 5 showed some possible resonance structures of 5-oxaporphyrin (isomers I−VI). The resonance structure I is most consistent with the above discussion based on the bond distances determined by X-ray crystallographic studies as well as the bond distances and the bond orders computed with ab initio molecular orbital theory. Moreover, the NBO charges of **3a** are shown in Figure S17 (Supporting Information). The C4 and C6 carbons were relatively cationic, and the Zn ion was the most cationic in the macrocycle of 5-oxaporphyrin. Therefore, the contribution from the resonance structure III is also significant.

X-ray structures of β-substituted 5-oxaporphyrin zinc complexes have been reported previously.[5c,8] Unfortunately, the reported 5-oxaporphyrin structures display orientational disorder that involves multiple sites for the oxa group, which obscures small variation in bond lengths in regions near the disordered oxa group. The structure of the β-octaethyl-5-oxaporphyrin cobalt complex was determined without such disorder, and it showed C−O bond distances of 1.340 and 1.348 Å and a C−O−C bond angle of 124.8°.[26] Bond angles of

dx.doi.org/10.1021/jo3010342 | J. Org. Chem. 2012, 77, 6510−6519

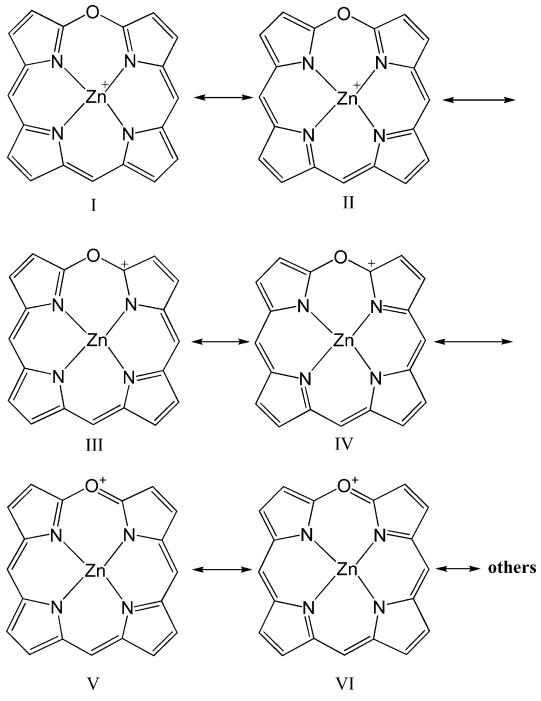

Figure 5. Resonance structures of 5-oxaporphyrin.

3a are listed in Table S3 (Supporting Information). The core geometry of **3a** is similar to that of the *β*-octaethyl-5-oxaporphyrin cobalt complex.

Alcoholysis of Oxaporphyrins and Its Selectivity. When the reaction of bilindione **2a** with $Ac_2O/Zn(OAc)_2$ was performed in 1% ethanol-containing chloroform, two products, 5-oxaporphyrin **3a** and a less polar blue compound, were obtained after acidic workup. ^{1}H NMR and TOF-mass spectroscopic data of the less polar blue compound suggested that it is 19-ethoxybilinone **8a**. If the reaction period was shorter than 30 min, unreacted **3a** was recovered (50% recovery), while bilinone **8a** was obtained as a major product in 61% yield in the longer reaction period. These observations suggest that **3a** is labile and reacted with a low concentration of ethanol.

Although (*β*-substituted-5-oxaporphyrinato)zinc(II) has been reported to react with various nucleophiles such as alkoxide, amide, or thiolate anions[4,27,28] to give a ring-opened product, bilinone, no reaction was reported with alcohols. As described below, 5-oxaporphyrin **3a** reacted even with MeOH, EtOH, *i*-PrOH, *t*-BuOH, and water, whose nucleophilicity should be very low.

The UV−vis spectral changes of **3a** in MeOH at 25 °C are shown in Figure 6. When **3a** was dissolved in MeOH, the absorption of **3a** at 388 and 639 nm decreased and new peaks appeared at 334 and 801 nm. The UV−vis spectral changes exhibited isosbestic points: it suggested that the reaction yielded only zinc bilinone **4a** exclusively. The MALDI TOF-MS spectrum of the product exhibited peaks at 808.4, 809.4, 810.4, 811.4, 812.4, 813.4, 814.2, and 815.4 (*m*/*z*), and the isotopic pattern was consistent with formation of both $C_{44}H_{32}N_4O_8Zn^+$ (M) and MH^+. Because 19-alkoxybilinone zinc complexes easily demetalated in dilute acid, it was difficult to isolate them with silica gel chromatography. After bilinone zinc complex **4a** was demetalated with 1 M HCl, the structure of 19-alkoxybilinone **7a** was confirmed by ^{1}H NMR, NOESY spectra, MALDI TOF-MS, and UV−vis spectroscopy. Compounds **7a**, **7c**, **8a**, and **9a**

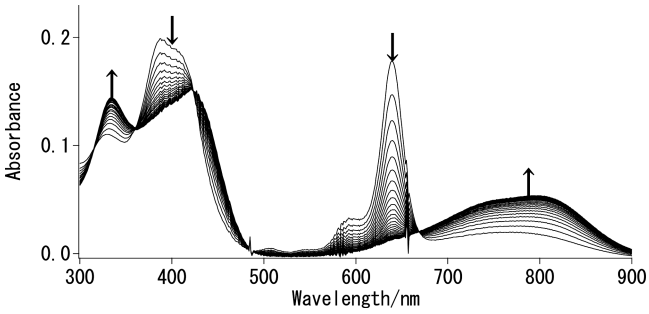

Figure 6. UV−vis spectral changes of 5.0×10^{-6} M of **3a** in MeOH at 298 K. Spectra were recorded every 1 min.

were also obtained in a preparative scale by the reaction of **3a** or **3c** with corresponding sodium alkoxide, and we confirmed that they were identical with those obtained in the solvolysis reactions. In the UV−vis spectrum, bilinone **7a** showed λ_{max} at 324, 404, and 645 nm in $CHCl_3$. The TOF-mass spectrum of **7a** showed a peak at 746 (M^+, M = $C_{44}H_{34}N_4O_8$). In the ^{1}H NMR, the resonances of pyrrole *β*-protons of bilinone **7a** appeared at 6.24, 6.28, 6.39, 6.54, 6.59, 6.81, 6.95, and 7.15 ppm and the phenyl ortho protons appeared at 7.62, 7.71, and 7.75 ppm. The resonances at 3.73 ppm (3H) and 3.96 ppm (9H) indicate that **7a** has four methoxy groups. The peak at 3.73 ppm is assigned to the 19-methoxy group and the peaks at 3.96 ppm are to the methyl ester groups in the phenyl groups. According to the NOESY spectra, following NOE correlations were found: the resonances of pyrrole *β*-protons at 6.54 and 7.15 ppm (H-7, H-3) with that of the ortho phenyl protons at 7.62 ppm, the resonances of pyrrole *β*-protons at 6.59 and 6.95 ppm (H-12, H-8) with that of the ortho phenyl protons at 7.75 ppm, and the resonances of pyrrole *β*-protons at 6.39 and 6.81 ppm (H-13, H-17) with that of the ortho phenyl proton at 7.71 ppm. Based on these NOESY correlations, we identified that bilinone **7a** had (4*Z*,9*Z*,15*Z*) configuration.

The first-order rate constants of the ring-opening reaction of **3a** in MeOH, EtOH, or *i*-PrOH at 30 °C were 0.0103, 0.075, and 0.0082 s^{-1}, respectively (Table 1 and Scheme 2). The half-lives of **3a** in these alcohols are in the range 10−90 s. By contrast, the spectral changes of 5-oxaporphyrin **3a** in *t*-BuOH and in water were very slow. The reactivity of **3a** toward alcohols is, thus, primary > secondary ≫ tertiary. Therefore, steric requirements of the transition state of the reaction are rather severe. These results demonstrate that the 5-oxaporphyrin can be used to functionalize hydroxy groups regioselectively. The reaction of carbenium ions with alcohols and water have been studied, where the reactivity decreases in the order: MeOH > EtOH > *i*-PrOH > H_2O > *t*-BuOH.[29] The ratio of the rate constant of reaction of a diphenylcarbenium ion with *i*-PrOH to that with *t*-BuOH is 4.5, while the ratio of the rates of reaction with **3a** was 2700. Therefore, selectivity of the reaction of **3a** with *sec*- and *tert*-alcohols is much higher than the diphenylcarbenium ion.

Conversion of iron 5-oxaporphyrin to bilindione attracts interest as a model reaction of verdoheme to biliverdin transformation catalyzed by heme oxygenase.[1b,5b,30] Although hydrolysis of 5-oxaporphyrin can yield bilindione, the enzymatic reaction proceeds with consumption of one O_2 molecule and four reducing equivalents.[1] As shown in Table 1, the reaction rate of **3a** with water is at least 2 orders of magnitude slower than that with MeOH. Low nucleophilicity of

dx.doi.org/10.1021/jo3010342 | J. Org. Chem. 2012, 77, 6510−6519

Table 1. First-Order Rate Constants of the Ring-Opening Reaction of 3a−c in MeOH, in EtOH, and in *i*-PrOH

solvent	k/s^{-1}, **3a** (COOMe)	k/s^{-1}, **3b** (OMe)	k/s^{-1}, **3c** (H)	T (K)
EtOH	$(7.5 \pm 0.5) \times 10^{-2}$	$(3.3 \pm 0.3) \times 10^{-3}$	$(1.1 \pm 0.1) \times 10^{-2}$	303
MeOH	$(1.03 \pm 0.03) \times 10^{-2}$	$(1.0 \pm 0.1) \times 10^{-3}$	$(2.2 \pm 0.1) \times 10^{-3}$	303
iso-PrOH	$(8.2 \pm 0.3) \times 10^{-3}$	$(8.7 \pm 0.3) \times 10^{-5}$	$(3.2 \pm 0.1) \times 10^{-4}$	303
t-BuOH	$(3.0 \pm 0.3) \times 10^{-6}$	*a*	*a*	303
H_2O[b]	$(8.6 \pm 1.0) \times 10^{-5}$	*a*	*a*	303
EtOH	$(5.8 \pm 0.1) \times 10^{-2}$	$(2.1 \pm 0.2) \times 10^{-3}$	$(9.0 \pm 0.2) \times 10^{-3}$	298
MeOH	$(4.6 \pm 0.1) \times 10^{-3}$	$(4.1 \pm 0.1) \times 10^{-4}$	$(7.8 \pm 0.8) \times 10^{-4}$	298

[a]Not determined. [b]Hydrolysis was performed in 5%(v/v) CH_3CN in water. Both the zinc complex of bilindione and the free base bilindione were formed.

Scheme 2. Synthetic Route to 19-Alkoxybilinone Zinc Complexes 4−6 and Their Free Bases 7−9[a]

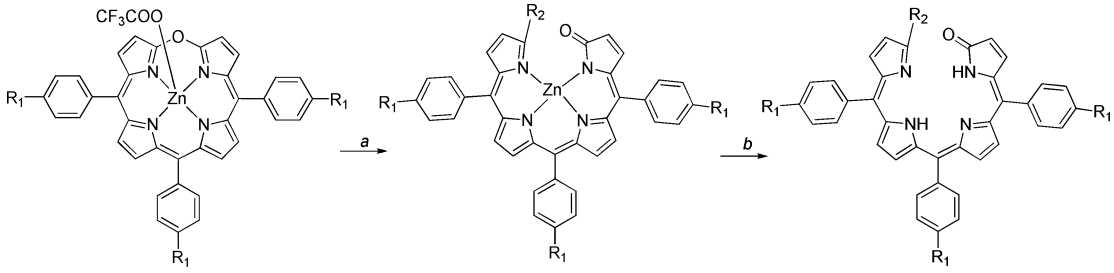

3a: R_1 = COOMe
3b: R_1 = OMe
3c: R_1 = H

4a: R_1 = COOMe, R_2 = OCH_3
4b: R_1 = OMe, R_2 = OCH_3
4c: R_1 = H, R_2 = OCH_3
5a: R_1 = COOMe, R_2 = OC_2H_5
5b: R_1 = OMe, R_2 = OC_2H_5
5c: R_1 = H, R_2 = OC_2H_5
6a: R_1 = COOMe, R_2 = $OCH(CH_3)_2$
6b: R_1 = OMe, R_2 = $OCH(CH_3)_2$
6c: R_1 = H, R_2 = $OCH(CH_3)_2$

7a: R_1 = COOMe, R_2 = OCH_3
7b: R_1 = OMe, R_2 = OCH_3
7c: R_1 = H, R_2 = OCH_3
8a: R_1 = COOMe, R_2 = OC_2H_5
8b: R_1 = OMe, R_2 = OC_2H_5
8c: R_1 = H, R_2 = OC_2H_5
9a: R_1 = COOMe, R_2 = $OCH(CH_3)_2$
9b: R_1 = OMe, R_2 = $OCH(CH_3)_2$
9c: R_1 = H, R_2 = $OCH(CH_3)_2$

[a]Reagents: (a) various alcohols R_2H; (b) 1 M HCl.

water could be one of reasons why the enzymatic transformation is not a simple hydrolysis but a redox reactions.

Mechanism of the Ring-Opening Reaction. Balch and co-workers[31] proposed that the ring-opening reaction of 5-oxaporphyrin with cyanide ion proceeds via a 4-cyano-5-oxaporphyrin intermediate, followed by the bond cleavage of C4−O5, to give 19-cyanobilinone. Recently theoretical calculations of the ring-opening reaction of oxaporphyrin with NH_2^-, NMe_2^-, OH^-, and CN^- have been reported.[32] According to the molecular orbital studies, an intermediate is initially formed by nucleophilic attack of the anions to C4, and it is then directly converted to a helical ring-opened zinc complex by passing through a transition state. This mechanism is schematically shown in Scheme 3 for the reaction with alcohols.

We calculated the energies of 4-alkoxy-5-oxaporphyrins **11** and 19-alkoxybilinones **12** by ab initio molecular orbital calculations at the B3LYP/6-31G(d) level. The optimized geometries are shown in Figure 7, and the energies are listed in Table 2. The energy (ΔE_1) of the MeOH adduct intermediate (**11d**) relative to the starting compounds was similar to that of the *i*-PrOH adduct intermediate (**11e**), while the energy of *t*-BuOH adduct intermediate (**11f**) was significantly higher. On the other hand, the energy (ΔE_2) of MeO-bilinone zinc complex (**12d**) is much lower than those of both *i*-PrO-

Scheme 3. Reaction of 5-Oxaporphyrin with Alcohol via Alcohol Adducts (11) To Afford 19-Alkoxybilinone Zinc Complexes (12)

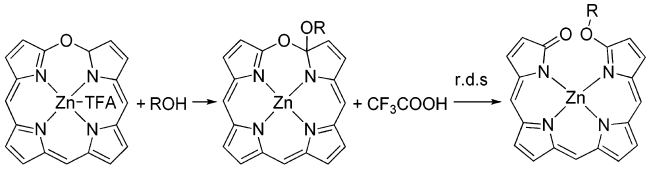

10

11d: R = Me
11e: R = Pr^i
11f: R = Bu^t

12d: R = Me
12e: R = Pr^i
12f: R = Bu^t

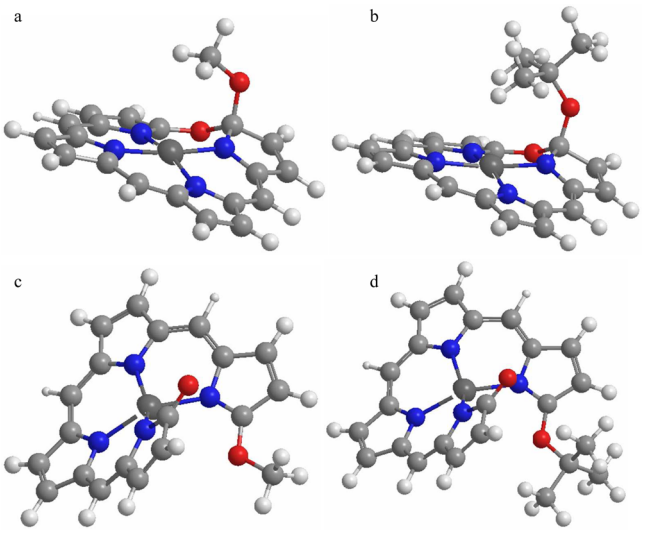

Figure 7. Optimized geometry of (a) **11d**, (b) **11f**, (c) **12d**, and (d) **12f** at the B3LYP/6-31G(d) level.

dx.doi.org/10.1021/jo3010342 | J. Org. Chem. 2012, 77, 6510−6519

Table 2. Energies of 5-Oxaporphyrin Alcohol Adduct Zinc Complexes (11) and 19-Alkoxybilinone Zinc Complexes (12) Calculated by ab Initio (B3LYP/6-31G(d))

	oxaporphyrin alcohol adduct (**11**) (au)	ΔE_1[a] (kcal mol^{-1})	19-alkoxybilinone (**12**) (au)	ΔE_2[b] (kcal mol^{-1})
MeOH	−2919.17727	24.1	−2919.20569	6.3
i-PrOH	−2997.81386	25.5	−2997.83848	10.1
t-BuOH	−3037.11831	33.8	−3037.15562	10.4

[a] $\Delta E_1 = E(\mathbf{11}) + E(CF_3COOH) - E(\mathbf{10}) - E(ROH)$. [b] $\Delta E_2 = E(\mathbf{12}) + E(CF_3COOH) - E(\mathbf{10}) - E(ROH)$.

bilinone zinc complex (**12e**) and *t*-BuO-bilinone zinc complex (**12f**). The rate constants listed in Table 1 indicate that the ring-opening reactions of **3a**−**c** with MeOH and *i*-PrOH have transition states in similar energies while the ring-opening reactions with *t*-BuOH have transition states with much higher energy. Therefore, the structures of alcohol adducts **11d**−**f** seem to be a good approximation of the transition state of these reactions.

Substituent Effects on the Reactivity of 5-Oxaporphyrins. The solvolysis reaction rates were compared for three 5-oxaporphyrins **3a**−**c** to investigate electronic effects of substituents on the ring-opening reaction rates. Table 1 summarizes the rate constants of solvolysis of **3a**−**c** in either MeOH, EtOH, or *i*-PrOH at 298 or 303 K. The Hammett plots for the rate constants of solvolysis of 5-oxaporphyrins are shown in Figure 8. The substituent constants σ_p were taken

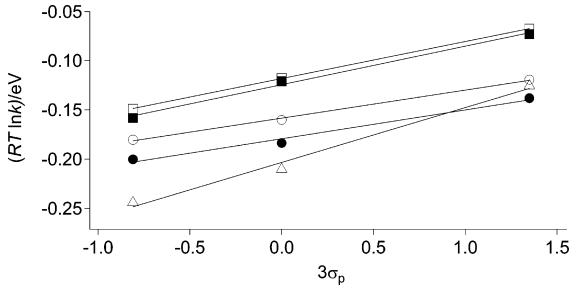

Figure 8. Hammett plots for the rate constants of the reaction of oxaporphyrins with MeOH (black circle, 298 K; white circle, 303 K), EtOH (black square, 298 K; white square, 303 K), and *i*-PrOH (white triangle, 303 K). ρ/eV = 0.039 ± 0.003 (EtOH at 298 K), 0.0375 ± 0.0004 (EtOH at 303 K), 0.029 ± 0.004 (MeOH at 298K), 0.028 ± 0.001 (MeOH at 303 K), and 0.056 ± 0.006 (*i*-PrOH at 303 K). σ_p (COOMe) = 0.45, σ_p (H) = 0, σ_p (OMe) = −0.27.

from the literatures and the value of σ_p (COOEt) was used in place of σ_p (COOMe).[33] Since all three phenyl rings of 5-oxaporphyrin are substituted, $3\sigma_p$ was used as the sum of the substituent constant. Figure 8 demonstrates that the solvolysis rates are linearly correlated with the substituent constants σ_p. The positive slopes indicate that a positive charge diminishes in the transition state. The Hammett reaction constants of the solvolysis of **3a** in MeOH and in EtOH at 298 K were 0.029 and 0.039 eV, respectively. Kadish et al. reported that the Hammett reaction constants ρ of the cation radical, dication, anion radical and dianion formation reactions of para-substituted tetraphenylporphyrins containing various metals in the center were in the range 0.05−0.09 eV.[34] Values of reaction constants of **3a**−**c** similar to those of one-electron transfer indicate that nearly unit positive charge should be diminished in the transition state of the reactions. The reaction mechanism that cationic 5-oxaporphyrin **10** is converted to a neutral adduct **11**, whose structure is similar to the transition state of the reaction, is thus supported by the Hammett plot.

The first-order rate constants of ring-opening reaction with alcohols were also determined in toluene. Table 3 summarizes the rate constants of the nucleophilic ring-opening reaction of **3a**−**c** by MeOH, EtOH, and *i*-PrOH at 303 K. In alcohols, the reactivity decreases in the order EtOH > MeOH > *i*-PrOH ≫ *t*-BuOH, while, in toluene, in the order MeOH ∼ EtOH > *i*-PrOH. When **3a** reacted with 1 M MeOH in acetonitrile at 303 K, the first-order rate constant of ring-opening reaction was (1.4 ± 0.2) × 10^{-4} s^{-1}. The first-order rate constant in toluene was about 5.4 times faster than in acetonitrile. A slower rate in the polar solvent is consistent with the reaction mechanism that a positive charge diminished in the transition state.

To compare the reactivity of *meso*-substituted oxaporphyrin with that of *β*-substituted one, [3,7-bis(2-acetoxyethyl)-21,23-didehydro-2,8,13,17-tetraethyl-12,18-dimethyl-23*H*-5-oxaporphyrinato](chloro)zinc(II) (**13**) was prepared by a previously reported method.[27a] The first order rate constant of the ring-opening reaction of **13** in EtOH at 30 °C was 0.00092 ± 0.00001 s^{-1}. Therefore, **13** is less reactive than **3a**, **3b**, and **3c**. The electron-donating ability of eight alkyl groups on the *β*-positions is thus stronger than three 4-methoxyphenyl groups in the *meso* positions. Molecular orbital calculations at B3LYP/6-31G indicated that the Mulliken atomic charges of C4 and C6 of [2,3,7,8,12,13,17,18-octamethyl-5-oxaporphyrinato]zinc(II), **3a**, and **3c** were 0.475, 0.494, and 0.493 respectively, showing that the C4, C6 carbons of **3a** and **3c** are more electrophilic.

UV−vis Absorption and Fluorescence Emission Spectra of 5-Oxaporphyrins. Figure 9 compares UV−vis spectra

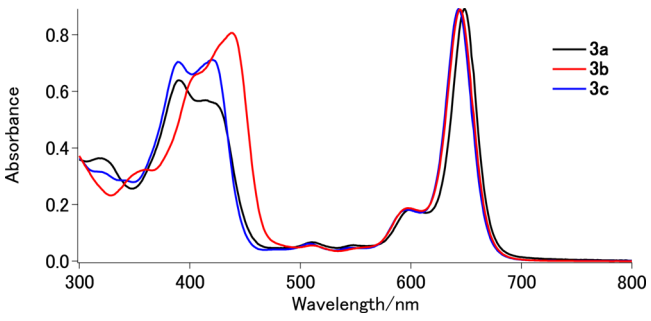

Figure 9. UV−vis spectra of oxaporphyrins **3a**−**c** in chloroform.

Table 3. First-Order Rate Constants of the Ring-Opening Reaction of 3a−c in 1 M MeOH, 1 M EtOH, and 1 M *i*-PrOH in Toluene at 30 °C

nucleophile	k (s^{-1}), **3a** (COOMe)	k (s^{-1}), **3b** (OMe)	k (s^{-1}), **3c** (H)
EtOH	(3.65 ± 0.04) × 10^{-4}	(7.0 ± 0.1) × 10^{-5}	(1.83 ± 0.05) × 10^{-4}
MeOH	(7.5 ± 0.1) × 10^{-4}	(7.3 ± 0.4) × 10^{-5}	(2.0 ± 0.1) × 10^{-4}
i-PrOH	(7.8 ± 0.4) × 10^{-5}	(1.17 ± 0.04) × 10^{-5}	(4.0 ± 0.4) × 10^{-5}

dx.doi.org/10.1021/jo3010342 | J. Org. Chem. 2012, 77, 6510−6519

of 5-oxaporphyrins **3a**–**c**. 5-Oxaporphyrin substituted with COOMe (**3a**) and unsubstituted phenyl groups (**3c**) exhibited similar absorption spectra, while 5-oxaporphyrin substituted with OMe (**3b**) showed a red-shifted B band.

To explore the electronic states, we performed time-dependent HF calculations of **3a**–**c** at the 6-31G(d,p) level, without an axial ligand. The geometry was optimized at the HF/6-31G(d,p) level. Absorption maxima, oscillator strengths, CI configurations, and the transition electric dipole moment directions are listed in Tables S7–S9 (Supporting Information). The simulated UV–vis spectra of **3a**–**c** based on the MO calculations are shown in Figure S18 (Supporting Information). These results indicate that the electron-donating OMe groups have significant effects on the electronic states of 5-oxaporphyrins. Table S10 (Supporting Information) lists selected MO energies of **3a**–**c**. The OMe substituents particularly destabilized the HOMO-1 orbital.

Fluorescence spectra of **3a**–**c** are shown in Figures 10 and 11, and spectroscopic data are listed in Tables 4 and 5. The

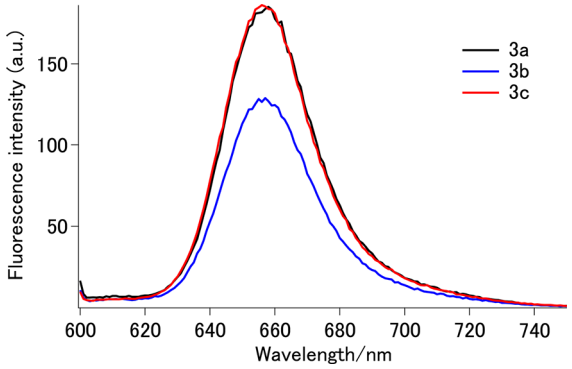

Figure 10. Fluorescence spectra of oxaporphyrin **3a**–**c** at 298 K in toluene where the samples were excited at 590 nm.

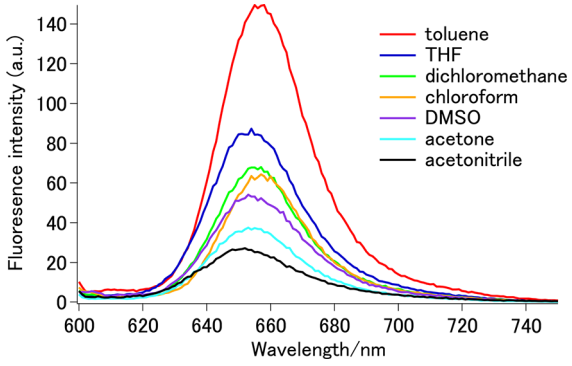

Figure 11. Fluorescence spectra of oxaporphyrin **3a** in various solvents at 298 K. The excitation wavelength was 590 nm.

Table 4. Fluorescence Data of Oxaporphyrins 3a–c in Toluene

	λ_{em} (nm)	λ_{abs} (nm)	Stokes shift (nm)	fluorescence quantum yield
3a (COOMe)	657	646	11	0.071
3b (OMe)	657	646	11	0.050
3c (H)	657	645	12	0.071

fluorescence quantum yield of **3a** in toluene was determined to be 0.071 by using tetraphenylporphyrin (ϕ = 0.13) as a reference compound.[35] The fluorescence quantum yields of **3b** and **3c** were 0.050 and 0.071, respectively. Compared to the fluorescence quantum yield of tetraphenylporphyrin zinc complex (ϕ = 0.033), the fluorescence quantum yields of 5-oxaporphyrins were higher.[35] Methoxy-substituted oxaporphyrin **3b** showed a lower fluorescence quantum yield than **3a** and **3c**. Fluorescence spectrum of **3a** showed a peak at 657 nm in nonpolar solvents and 653 nm in polar solvents (Table 5). Fluorescence intensity was higher in nonpolar solvents than in polar solvents as shown in Figure 11. Stokes shifts of **3a** were 8 to 15 nm and they were smaller than that of the porphyrin zinc complex. Excitation of the Soret band at 400 nm also resulted in the fluorescence at 657 nm, although the fluorescence quantum yield was significantly lower.

Table 5. Fluorescence Data of Oxaporphyrin 3a in Various Solvents

solvent	λ_{em} (nm)	λ_{abs} (nm)	Stokes shift (nm)	rel fluorescence intensity
toluene	657	646	11	4.84
THF	653	642	11	2.92
CH_2Cl_2	657	645	12	2.18
$CHCl_3$	657	649	8	2.00
DMSO	653	642	11	1.85
acetone	653	641	12	1.26
CH_3CN	653	638	15	1.00

CONCLUSION

meso-Triarylbilindiones were converted into [*meso*-triaryl-21,23-didehydro-23*H*-5-oxaporphyrinato]zinc(II) by refluxing them with acetic anhydride and zinc acetate in chloroform, and they were isolated as a CF_3COO^- salt. X-ray crystallographic studies revealed that the CF_3COO^- is coordinated to the zinc. In spite of its ionic structure, it is soluble in most of the organic solvents, and the solubility in toluene was higher than *meso*-tetraphenylporphyrin and *β*-octaethylporphyrin. Substituent effects on the reactivity and spectroscopic properties were studied for three [21,23-didehydro-23*H*-5-oxaporphyrinato]-zinc(II) complexes. [*meso*-Triaryl-21,23-didehydro-23*H*-5-oxaporphyrinato]zinc(II) is labile toward nucleophiles than [*β*-octaalkyl-5-oxaporphyrinato]zinc(II) and reacted with weak nucleophiles such as methanol, ethanol, and 2-propanol to give bilinone zinc complexes having near-infrared absorption at 800 nm. The positive Hammett reaction constants for COOMe, H, and OMe substituents in the phenyl rings are consistent with a neutral adduct formation from the cationic reactant. Solvolysis of [*meso*-triaryl-21,23-didehydro-23*H*-5-oxaporphyrinato]zinc-(II) occurs rapidly in primary and secondary alcohols while that in tertiary alcohol and water was slower by a factor of 10^2 to 10^3. The electron-donating substituents in the aryl groups caused a significant red shift in electronic spectra, and the fluorescence quantum yield was lower than that of [*meso*-triphenyl-21,23-didehydro-23*H*-5-oxaporphyrinato]zinc(II), while the electron-withdrawing substituents showed minor effects on the electronic spectrum and the fluorescence spectrum. Finally, [*meso*-triaryl-21,23-didehydro-23*H*-5-oxaporphyrinato]zinc(II) is a fluorescent electrophile, easily converted to the helical compound having near-infrared absorption, and would find various applications to new functional materials.

dx.doi.org/10.1021/jo3010342 | J. Org. Chem. 2012, 77, 6510–6519

EXPERIMENTAL SECTION

Molecular orbital calculations were performed using Gaussian 09 (Gaussian Inc.).[36] Commercially available reagents were used as received. Chromatographic separations of 5-oxaporphyrins and bilinones were performed using silica gel 60N, spherical neutral with particle size 40−50 μm. Ethanol-free chloroform was used to prepare 5-oxaporphyrin. Preparation of bilindiones **2a**, **2b**, and **2c** was reported elsewhere.[14a,c] Tetramethylsilane was used as an internal standard of ^{1}H and ^{13}C NMR spectra, and benzotrifluoride was used as an internal standard (−63.7 ppm) of ^{19}F NMR spectra. Assignments of ^{1}H NMR and ^{13}C NMR were performed using ^{1}H−^{1}H COSY, NOESY, HMBC, and HMQC spectra. A green plate crystal of 5-oxaporphyrin **3a** was obtained by slow diffusion of cyclohexane to a solution of **3a** in toluene. Crystal data and data collection parameters are given in Table 6.

Table 6. Crystallographic Data for Oxaporphyrin 3a

formula	$C_{50}H_{29}F_3N_4O_9Zn$	V, Å^3	4446.99(16)
formula wt	952.14	Z	4
color and habit	green plate	T, K	113(2)
crystal system	monoclinic	d_{calcd} (mg cm^{-3})	1.422
space group	$P2_1/n$	radiation (λ, Å)	Cu K_α (1.54187)
a, Å	21.2044(4)	μ, mm^{-1}	1.415
b, Å	10.4376(2)	range of transmission factors	0.6683 to 0.7448
c, Å	21.7778(5)	$R_1{}^a$	0.0852
α deg	90	$wR_2{}^b$	0.2359
β, deg	112.6870(10)	GOF	0.986
γ, deg	90		

$^aR_1 = \sum||F_o| - |F_c||/\sum|F_o|$. ^{b}wR2 $= [\sum[w(F_o^2 - F_c^2)^2]/\sum[w(F_o^2)^2]]^{1/2}$.

[21,23-Didehydro-10,15,20-tris(4-methoxycarbonylphenyl)-23*H*-5-oxaporphyrinato](trifluoroacetato)zinc(II) (3a). A solution of bilindione **2a** (23.2 mg, 0.0313 mmol), zinc acetate (11.0 mg, 0.0546 mmol), and acetic anhydride (0.6 mL, 6.35 mmol) in amylene-stabilized chloroform (100 mL) was refluxed for 1 h. After being cooled to room temperature, the reaction mixture was washed with water twice, and the organic layer was dried over Na_2SO_4. Evaporation of the solvent under reduced pressure gave a green solid. The product was purified on silica gel chromatography using CH_2Cl_2/acetone/trifluoroacetic acid (20:1:0.1) as eluent. The green fractions were combined, washed with water, dried over Na_2SO_4, and evaporated to yield 27.9 mg of **3a** in a quantitative yield. ^{1}H NMR (500 MHz, chloroform-*d*): δ = 4.04 (s, 3H; CH_3), 4.06 (s, 6H; CH_3), 7.76 (d, J = 4.45 Hz, 2H; pyrrole H-12), 7.92 (d, J = 4.45 Hz, 2H; pyrrole H-13), 7.94−8.06 (m, 6H; 10,15,20-phenylene H-2′), 8.09 (d, J = 4.75 Hz, 2H; pyrrole H-3), 8.22 (d, J = 4.75 Hz, 2H; pyrrole H-2), 8.31 (d, J = 8.45 Hz, 2H; 15-phenylene H-3′), 8.34 ppm (d, J = 8.45 Hz, 4H; 10,20-phenylene H-3′). ^{13}C NMR (125 MHz, chloroform-*d*): δ = 52.50 (CH_3), 52.53 (CH_3), 120.0 (pyrrole C-3), 128.2 (phenylene C-3′), 128.5 (phenylene C-3′), 130.6 (meso), 130.8 (pyrrole C-12), 132.4−133.8 (phenylene C-2′), 134.5 (pyrrole C-13), 135.9 (meso), 138.6 (pyrrole C-2), 140.7, 143.0, 143.8 (pyrrole C-1), 144.3, 150.0 (pyrrole C-14), 154.6 (pyrrole C-11), 165.4 (pyrrole C-4), 166.76 (C═O), 166.81 ppm (C═O). ^{19}F NMR (471 MHz, chloroform-*d*): δ = −75.4 ppm (CF_3COO). MS (MALDI-TOF): m/z = 777 [M − CF_3COO]$^+$. HRMS (FAB): calcd for $C_{43}H_{29}O_7N_4{}^{64}Zn$ m/z 777.1328, found 777.1344. UV−vis (CH_2Cl_2, 25 °C): λ_{max} (ε_{max}) 323 (2.13 × 10^4), 391 (3.89 × 10^4), 601 (1.05 × 10^4), 644 nm (4.57 × 10^4 M^{-1} cm^{-1}).

[21,23-Didehydro-10,15,20-tris(4-methoxyphenyl)-23*H*-5-oxaporphyrinato](trifluoroacetato)zinc(II) (3b). A solution of bilindione **2b** (4.5 mg, 0.0072 mmol), zinc acetate (2.6 mg, 0.014 mmol), and acetic anhydride (0.14 mL, 1.5 mmol) in amylene-stabilized chloroform (25 mL) was refluxed for 1 h. After being cooled to room temperature, the reaction mixture was washed with water twice, and the organic layer was dried over Na_2SO_4. Evaporation of the solvent under reduced pressure gave a green solid. The product was purified on silica gel chromatography using CH_2Cl_2/acetone/trifluoroacetic acid (20:1:0.1) as eluent. The green fractions were combined, washed with water, dried over Na_2SO_4, and evaporated to yield 4.2 mg of **3b** (72%). ^{1}H NMR (500 MHz, acetone-d_6): δ = 4.04 (s, 3H; CH_3), 4.05 (s, 6H; CH_3), 7.29−7.33 (t, J = 8.60 Hz, 6H; phenyl), 7.83 (d, J = 4.60 Hz, 2H; pyrrole), 7.84−7.92 (d, J = 4.75 Hz, 6H; phenyl), 8.00 (d, J = 4.60 Hz, 2H; pyrrole), 8.16 (d, J = 4.60 Hz, 2H; pyrrole), 8.31 ppm (d, J = 4.60 Hz, 2H; pyrrole). ^{13}C NMR (125 MHz, chloroform-*d*): δ = 55.5 (CH_3), 112.0, 118.8, 130.7, 131.0, 132.5, 134.5, 134.9, 137.4, 138.8, 142.3, 143.8, 150.6, 155.1, 160.2, 160.3, 164.9, 166.76, 166.81 ppm. ^{19}F NMR (471 MHz, chloroform-*d*): δ = −75.5 ppm (CF_3COO). MS (MALDI-TOF): m/z = 693 [M-CF_3COO]$^+$; HRMS (FAB): calcd for $C_{40}H_{29}O_4N_4{}^{64}Zn$ m/z 693.1480, found 693.1454. UV−vis (CH_2Cl_2, 25 °C): λ_{max} (ε_{max}) 437 (6.08 × 10^4), 587 (1.22 × 10^4), 643 nm (6.42 × 10^4 M^{-1} cm^{-1}).

[21,23-Didehydro-10,15,20-triphenyl-23*H*-5-oxaporphyrinato](trifluoroacetato)zinc(II) (3c). A solution of bilindione **2c** (16.5 mg, 0.0296 mmol), zinc acetate (11.0 mg, 0.0546 mmol), and acetic anhydride (0.6 mL, 6.35 mmol) in amylene-stabilized chloroform (100 mL) was refluxed for 1 h. After being cooled to room temperature, the reaction mixture was washed with water twice, and the organic layer was dried over Na_2SO_4. Evaporation of the solvent under reduced pressure gave a green solid. The product was purified on silica gel chromatography using CH_2Cl_2/acetone/trifluoroacetic acid (20:1:0.1) as eluent. The green fractions were combined, washed with water, dried over Na_2SO_4, and evaporated to yield 14.1 mg of **3c** (66.5%). ^{1}H NMR (500 MHz, dichloromethane-d_2): δ = 7.63−7.74 (m, 9H; phenyl), 7.82 (d, J = 4.60 Hz, 2H; pyrrole), 7.84−7.95 (m, 6H; phenyl), 7.98 (d, J = 4.60 Hz, 2H; pyrrole), 8.05 (d, J = 4.50 Hz, 2H; pyrrole), 8.25 ppm (d, J = 4.50 Hz, 2H; pyrrole). ^{13}C NMR (125 MHz, chloroform-*d*): δ = 112.8, 126.8−127.4, 128.7, 128.8, 130.7, 132.5−133.4, 134.5, 137.2, 138.6, 138.8, 140.0, 142.0, 143.8, 150.4, 155.0, 165.1 ppm. ^{19}F NMR (471 MHz, chloroform-*d*): δ = −75.4 ppm (CF_3COO). MS (MALDI-TOF): m/z = 603 [M − CF_3COO]$^+$. HRMS (FAB): calcd for $C_{37}H_{23}ON_4{}^{64}Zn$ m/z 603.1163, found 603.1142. UV−vis (CH_2Cl_2, 25 °C): λ_{max} (ε_{max}) 388 (4.80 × 10^4), 415 (5.52 × 10^4), 587 (1.03 × 10^4), 641 nm (5.44 × 10^4 M^{-1}cm^{-1}).

(4*Z*,9*Z*,15*Z*)-1,21-Dihydro-19-methoxy-5,10,15-tris(4-methoxycarbonylphenyl)-23*H*-bilin-1-one (7a). A solution of oxaporphyrin **3a** (11.5 mg, 0.0129 mmol) and sodium methoxide (3.0 mg, 0.0555 mmol) in anhydrous methanol (30 mL) was stirred at room temperature for 30 min. The reaction mixture was quenched by 10% NH_4Cl (20 mL), and chloroform (50 mL) was added. The chloroform solution was washed with 1 M HCl twice and washed with water, and the organic layer was dried over Na_2SO_4. Evaporation of the solvent under reduced pressure gave a blue solid. The product was purified on silica gel chromatography using chloroform as eluent to yield 5.3 mg of **7a** (55.3%). ^{1}H NMR (500 MHz, acetone-d_6): δ = 3.73 (s, 3H; OCH_3), 3.96 (m, 9H; $COOCH_3$), 6.24 (d, J = 4.80 Hz, 1H; pyrrole H-18), 6.28 (d, J = 4.60 Hz, 1H; pyrrole H-2), 6.39 (d, J = 4.15 Hz, 1H; pyrrole H-13), 6.54 (d, J = 4.15 Hz, 1H; pyrrole H-7), 6.59 (s, 1H; pyrrole H-12), 6.81 (d, J = 4.80 Hz, 1H; pyrrole H-17), 6.95 (d, J = 4.15 Hz, 1H; pyrrole H-8), 7.15 (d, J = 5.50 Hz, 1H; pyrrole H-3), 7.62 (d, J = 8.25 Hz, 2H; 5-phenylene H-2′), 7.71 (d, J = 8.25 Hz, 2H; 15-phenylene H-2′), 7.75 (d, J = 7.55 Hz, 2H; 10-phenylene H-2′), 8.13−8.34 (m, 6H; 5,10,15-phenylene H-3′), 10.27 (s, 1H; NH), 13.06 ppm (s, 1H; NH). ^{13}C NMR (125 MHz, chloroform-*d*): δ = 52.30 ($COOCH_3$), 52.36 ($COOCH_3$), 52.41 ($COOCH_3$), 55.7 (OCH_3), 117.3, 119.7 (pyrrole C-13), 120.2 (pyrrole C-18), 123.8, 125.6 (pyrrole C-2), 127.8 (pyrrole C-7), 129.09, 129.14, 129.3, 129.6, 130.0, 130.2, 131.0, 131.1, 131.2, 132.1, 134.9 (pyrrole C-8), 136.58, 136.64 (pyrrole C-3), 138.3, 138.8 (pyrrole C-17), 141.1, 141.2, 141.4, 141.8, 142.3 (pyrrole C-4), 149.1 (pyrrole C-16), 151.9 (pyrrole C-9), 166.58 ($COOCH_3$), 166.66 ($COOCH_3$), 166.74 ($COOCH_3$), 166.79

dx.doi.org/10.1021/jo3010342 | J. Org. Chem. 2012, 77, 6510−6519

(pyrrole C-6), 170.2 (pyrrole C-1), 177.1 ppm (pyrrole C-19). MS (MALDI-TOF): m/z = 746 $[M]^+$. HRMS (FAB): calcd for $C_{44}H_{34}O_8N_4$ m/z 746.2377, found 746.2356. UV−vis ($CHCl_3$, 25 °C): λ_{max} (ε_{max}) 324 (3.69×10^4), 404 (4.36×10^4), 645 nm (1.90×10^4 M^{-1} cm^{-1}).

(4*Z*,9*Z*,15*Z*)-1,21-Dihydro-19-methoxy-5,10,15-triphenyl-23*H*-bilin-1-one (7c). ^{1}H NMR (500 MHz, chloroform-*d*): δ = 3.63 (s, 3H; OCH_3), 6.18 (d, J = 4.75 Hz, 1H), 6.21 (d, J = 5.50 Hz, 1H), 6.43 (bs, 1H), 6.50 (d, J = 4.15 Hz, 1H), 6.61 (bs, 1H), 6.87 (d, J = 4.75 Hz, 1H), 6.84 (d, J = 3.45 Hz, 1H), 7.03 (d, J = 5.45 Hz, 1H), 7.38−7.57 (m, 15H), 10.18 ppm (s, 1H; NH), 12.83 ppm (s, 1H; NH). ^{13}C NMR (125 MHz, chloroform-*d*): δ =55.7, 118.7, 119.3, 119.9, 123.7, 124.9, 127.5, 127.76, 127.83, 128.0, 128.2, 128.4, 129.5, 130.6, 131.1, 131.3, 132.2, 134.8, 136.4, 136.6, 136.9, 137.0, 137.9, 138.5, 140.2, 141.1, 148.8, 152.0, 166.7, 170.3, 176.5 ppm. MS (MALDI-TOF): m/z = 572 $[M]^+$. HRMS (FAB): calcd for $C_{38}H_{28}O_2N_4$ m/z 572.2212, found 572.2200. UV−vis ($CHCl_3$, 25 °C): λ_{max} (ε_{max}) 328 (3.09×10^4), 402 (4.45×10^4), 637 nm (2.05×10^4 M^{-1} cm^{-1}).

(4*Z*,9*Z*,15*Z*)-1,21-Dihydro-19-ethoxy-5,10,15-tris(4-methoxycarbonylphenyl)-23*H*-bilin-1-one (8a). ^{1}H NMR (500 MHz, chloroform-*d*): δ = 1.11 (t, J = 6.90 Hz, 3H; CH_3), 3.97 (m, 9H; $COOCH_3$), 4.07 (bs, 2H; OCH_2), 6.18 (d, J = 4.60 Hz, 1H), 6.26 (d, J = 5.75 Hz, 1H), 6.34 (bs, 1H), 6.47 (d, J = 4.60 Hz, 1H), 6.54 (bs, 1H), 6.79 (d, J = 5.15 Hz, 1H), 6.84 (d, J = 5.15 Hz, 1H), 7.00 (d, J = 5.75 Hz, 1H), 7.48 (d, J = 8.00 Hz, 2H), 7.63 (m,, 4H), 8.12−8.15 (m, 6H), 10.27 (s, 1H; NH), 12.89 ppm (s, 1H; NH). ^{13}C NMR (125 MHz, chloroform-*d*): δ = 14.7, 52.3, 52.4, 64.7, 117.4, 119.6, 120.6, 123.9, 125.8, 127.7, 128.9, 129.1, 129.6, 130.0, 130.2, 131.1, 131.4, 132.1, 134.9, 136.5,135.6, 138.0, 138.9, 141.1, 141.4, 141.6, 141.8, 142.4, 149.4, 151.9, 166.6, 166.7, 166.8, 170.3, 176.7 ppm. MS (MALDI-TOF): m/z = 760 $[M]^+$. HRMS (FAB): calcd for $C_{45}H_{36}O_8N_4$ m/z 760.2533, found 760.2551. UV−vis ($CHCl_3$, 25 °C): λ_{max} (ε_{max}) 326 (3.90×10^4), 401 (4.82×10^4), 650 nm (1.99×10^4 M^{-1} cm^{-1}).

(4*Z*,9*Z*,15*Z*)-1,21-Dihydro-5,10,15-tris(4-methoxycarbonylphenyl)-19-(1-methylethoxy)-23*H*-bilin-1-one (9a). ^{1}H NMR (500 MHz, acetone-d_6): δ = 1.13 (d, J = 5.75 Hz 6H; CH_3), 3.95 (m, 9H; $COOCH_3$), 4.88 (m, 1H; CH), 6.19 (d, J = 4.60 Hz, 1H), 6.28 (dd, J = 5.75 Hz, 1.70 Hz, 1H), 6.34 (dd, J = 4.60 Hz, 2.3 Hz, 1H), 6.55 (d, J = 4.60 Hz, 1H), 6.59 (bs, 1H), 6.78 (d, J = 4.60 Hz, 1H), 6.93 (d, J = 4.60 Hz, 1H), 7.19 (dd, J = 5.75 Hz, 1.70 Hz, 1H), 7.64 (d, J = 8.00 Hz, 2H), 7.70 (d, J = 8.00 Hz, 2H), 7.73 (d, J = 8.00 Hz, 2H), 8.15−8.19 (m, 6H), 10.57 (s, 1H; NH), 12.87 ppm (s, 1H; NH). ^{13}C NMR (125 MHz, chloroform-*d*): δ = 22.0, 52.4, 72.4, 117.4, 121.1, 123.9, 125.7, 127.6, 129.1, 129.5, 130.1, 131.1, 131.3, 131.4, 132.2, 134.7, 136.4, 136.6, 137.8, 139.0, 141.0, 141.1, 141.4, 141.8, 149.6, 152.0, 166.6, 166.7, 166.8, 170.6, 176.0 ppm. MS (MALDI-TOF): m/z = 774 $[M]^+$, 731 $[M - CH(CH_3)_2]^+$. HRMS (FAB): calcd for $C_{46}H_{38}O_8N_4$ m/z 774.2690, found 774.2692. UV−vis ($CHCl_3$, 25 °C): λ_{max} (ε_{max}) 324 (3.68×10^4), 401 (4.29×10^4), 648 nm (2.28×10^4 M^{-1} cm^{-1}).

■ ASSOCIATED CONTENT

Ⓢ Supporting Information

^{1}H NMR of **3a**−**c**, **7a**,**c**, **8a**, and **9a**; ^{13}C NMR of **3a**−**c**, **7a**,**c**, **8a**, and **9a**; NOESY NMR of **7a**; UV−vis and MS spectral data of **4a**−**c**, **5**−**c**, **6a**−**c**, **7b**, **8b**,**c**, and **9b**,**c**; CIF file of **3a**; selected bond distances of **3a**; selected bond angles of **3a**; bond order of **3a**; atomic coordinates of **3a**−**c** optimized at the B3LYP/6-31G(d) level; NBO charges of **3a**; time-dependent RHF/6-31G(d,p)//RHF/6-31G(d,p) calculations of the excited states of **3a**−**c**; selected MO energies (eV) of oxaporphyrins **3a**−**c**. This material is available free of charge via the Internet at http://pubs.acs.org.

■ AUTHOR INFORMATION

Corresponding Author

*E-mail: tmizutan@mail.doshisha.ac.jp.

Notes

The authors declare no competing financial interest.

■ ACKNOWLEDGMENTS

This work was supported by "Creating Research Center for Advanced Molecular Biochemistry", Strategic Development of Research Infrastructure for Private Universities, the Ministry of Education, Culture, Sports, Science and Technology (MEXT), Japan.

■ REFERENCES

(1) (a) Ortiz de Montellano, P. R. *Curr. Opin. Chem. Biol.* **2000**, *4*, 221−227. (b) Yoshida, T.; Migita, C. T. *J. Inorg. Biochem.* **2000**, *82*, 33−41. (c) Zhu, Y.; Silverman, R. B. *Biochemistry* **2008**, *47*, 2231−2243. (d) Matsui, T.; Unno, M.; Ikeda-Saito, M. *Acc. Chem. Res.* **2010**, *43*, 240−247.

(2) Jackson, A. H.; Kenner, G. W.; Smith, K. M. *J. Chem. Soc. C* **1968**, 302−310.

(3) Saito, S.; Itano, H. A. *J. Chem. Soc., Perkin Trans. 1* **1986**, 1−7.

(4) (a) Fuhrhop, J. H.; Besecke, S.; Subramanian, J.; Mengersen, C.; Riesner, D. *J. Am. Chem. Soc.* **1975**, *97*, 7141−7152. (b) Fuhrhop, J. H.; Salek, A.; Subramanian, J.; Mengersen, C.; Besecke, S. *Liebigs Ann. Chem.* **1975**, 1131−1147.

(5) (a) Lagarias, J. C. *Biochim. Biophys. Acta* **1982**, *717*, 12−19. (b) Saito, S.; Itano, H. A. *Proc. Natl. Acad. Sci. U.S.A.* **1982**, *79*, 1393−1397. (c) Balch, A. L.; Latos-Grazynski, L.; Noll, B. C.; Olmstead, M. M.; Szterenberg, L.; Safari, N. *J. Am. Chem. Soc.* **1993**, *115*, 1422−1429. (d) Balch, A. L.; Latos-Grazynski, L.; Noll, B. C.; Olmstead, M. M.; Safari, N. *J. Am. Chem. Soc.* **1993**, *115*, 9056−9061. (e) Balch, A. L.; Koerner, R.; Latos-Grazynski, L.; Lewis, J. E., St.; Claire, T. N.; Zovinka, E. P. *Inorg. Chem.* **1997**, *36*, 3892−3897. (f) Claire, T. N. S.; Balch, A. L. *Inorg. Chem.* **1999**, *38*, 684−691.

(6) (a) Balch, A. L.; Mazzanti, M.; Olmstead, M. M. *J. Chem. Soc., Chem. Commun.* **1994**, 269−270. (b) Chang, C. K.; Aviles, G.; Bag, N. *J. Am. Chem. Soc.* **1994**, *116*, 12127−12128.

(7) Ali, H.; van Lier, J. E. *Tetrahedron Lett.* **1997**, *38*, 8173−8176.

(8) (a) Fuhrhop, J. H.; Krueger, P.; Sheldrick, W. S. *Justus Liebigs Ann. Chem.* **1977**, 339−359. (b) Fuhrhop, J. H.; Krueger, P. *Justus Liebigs Ann. Chem.* **1977**, 360−370. (c) Balch, A. L.; Olmstead, M. M.; Safari, N. *Inorg. Chem.* **1993**, *32*, 291−296.

(9) Hempenius, M. A.; Koek, J. H.; Lugtenburg, J.; Fokkens, R. *Recl. Trav. Chim. Pays-Bas* **1987**, *106*, 105−112.

(10) Latos-Grazynski, L.; Wojaczynski, J.; Koerner, R.; Johnson, J. J.; Balch, A. L. *Inorg. Chem.* **2001**, *40*, 4971−4977.

(11) Mizutani, T.; Sakai, N.; Yagi, S.; Takagishi, T.; Kitagawa, S.; Ogoshi, H. *J. Am. Chem. Soc.* **2000**, *122*, 748−749.

(12) Hamakubo, K.; Yagi, S.; Nakazumi, H.; Mizutani, T.; Kitagawa, S. *Tetrahedron Lett.* **2005**, *46*, 7151−7154.

(13) (a) Koerner, R.; Latos-Grazynski, L.; Balch, A. L. *J. Am. Chem. Soc.* **1998**, *120*, 9246−9255. (b) Latos-Grazynski, L.; Johnson, J.; Attar, S.; Olmstead, M. M.; Balch, A. L. *Inorg. Chem.* **1998**, *37*, 4493−4499.

(14) (a) Yamauchi, T.; Mizutani, T.; Wada, K.; Horii, S.; Furukawa, H.; Masaoka, S.; Chang, H.-C.; Kitagawa, S. *Chem. Commun.* **2005**, 1309−1311. (b) Asano, N.; Uemura, S.; Kinugawa, T.; Akasaka, H.; Mizutani, T. *J. Org. Chem.* **2007**, *72*, 5320−5326. (c) Nakamura, R.; Kakeya, K.; Furuta, N.; Muta, E.; Nishisaka, H.; Mizutani, T. *J. Org. Chem.* **2011**, *76*, 6108−6115.

(15) (a) Phillippi, M. A.; Goff, H. M. *J. Am. Chem. Soc.* **1982**, *104*, 6026−6034. (b) Kadish, K. M.; Cornillon, J. L.; Cocolios, P.; Tabard, A.; Guilard, R. *Inorg. Chem.* **1985**, *24*, 3645−3649. (c) Vitols, S. E.; Kumble, R.; Blackwood, M. E., Jr.; Roman, J. S.; Spiro, T. G. *J. Phys. Chem.* **1996**, *100*, 4180−7. (d) Watanabe, J.; Setsune, J. *Organometallics* **1997**, *16*, 3679−3683. (e) Satoh, M.; Ohba, Y.; Yamauchi, S.; Iwaizumi, M. *Inorg. Chem.* **1992**, *31*, 298−303.

(16) Dechaine, G. P.; Maham, Y.; Tan, X.; Gray, M. R. *Energy Fuels* **2011**, *25*, 737−746.
(17) (a) Lindsey, J. S.; Bocian, D. F. *Acc. Chem. Res.* **2011**, *44*, 638−650. (b) Hains, A. W.; Liang, Z.; Woodhouse, M. A.; Gregg, B. A. *Chem. Rev.* **2010**, *110*, 6689−6735. (c) Drain, C. M.; Varotto, A.; Radivojevic, I. *Chem. Rev.* **2009**, *109*, 1630−1658. (d) Imahori, H. *J. Mater. Chem.* **2007**, *17*, 31−41. (e) Matsui, E.; Matsuzawa, N. N.; Harnack, O.; Yamauchi, T.; Hatazawa, T.; Yasuda, A.; Mizutani, T. *Adv. Mater.* **2006**, *18*, 2523−2528.
(18) (a) Ruediger, W.; Thuemmler, F. *Angew. Chem., Int. Ed.* **1991**, *30*, 1216−1228. (b) Mroginski, M. A.; Murgida, D. H.; Hildebrandt, P. *Acc. Chem. Res.* **2007**, *40*, 258−266. (c) Inomata, K. *Bull. Chem. Soc. Jpn.* **2008**, *81*, 25−59. (d) Bongards, C.; Gaertner, W. *Acc. Chem. Res.* **2010**, *43*, 485−495.
(19) Mizutani, T.; Yagi, S. *J. Porphyrins Phthalocyanines* **2004**, *8*, 226−237.
(20) (a) Gouterman, M. Spectra of Porphyrin. *J. Mol. Spectrosc.* **1961**, *6*, 138−163. (b) Dorough, G. D.; Miller, J. R.; Huennekens, F. M. *J. Am. Chem. Soc.* **1951**, *73*, 4315−4320.
(21) (a) Toyota, K.; Hasegawa, J.; Nakatsuji, H. *Chem. Phys. Lett.* **1996**, *250*, 437−442. (b) Petit, L.; Quartarolo, A.; Adamo, C.; Russo, N. *J. Phys. Chem. B* **2006**, *110*, 2398−2404.
(22) Jursic, B. S. *THEOCHEM* **1998**, *454*, 105−116.
(23) Doerksen, R. J.; Thakkar, A. J. *Int. J. Quantum Chem.* **2002**, *90*, 534−540.
(24) Bak, B.; Christensen, D.; Dixon, W. B.; Hansen-Nygaard, L.; Andersen, J. R.; Schottländer, M. *J. Mol. Spectrosc.* **1962**, *9*, 124−129.
(25) Schomaker, V.; Pauling, L. *J. Am. Chem. Soc.* **1939**, *61*, 1769−1770.
(26) Balch, A. L.; Mazzanti, M.; Claire., T. N. S.; Olmstead, M. M. *Inorg .Chem.* **1995**, *34*, 2194−2220.
(27) (a) Mizutani, T.; Yagi, S.; Honmaru, A.; Murakami, S.; Furusyo, M.; Takagishi, T.; Ogoshi, H. *J. Org. Chem.* **1998**, *63*, 8769−8784. (b) Mizutani, T.; Yagi, S.; Morinaga, T.; Nomura, T.; Takagishi, T.; Kitagawa, S.; Ogoshi, H. *J. Am. Chem. Soc.* **1999**, *121*, 754−759. (c) Yagi, S.; Sakai, N.; Yamada, R.; Takahashi, H.; Mizutani, T.; Takagishi, T.; Kitagawa, S.; Ogoshi, H. *Chem. Commun.* **1999**, 911−912.
(28) Johnson, J. A.; Olmstead, M. M.; Balch, A. L. *Inorg. Chem.* **1999**, *38*, 5379−5383.
(29) (a) Bartl, J.; Steenken, S.; Mayr, H. *J. Am. Chem. Soc.* **1991**, *113*, 7710−7716. (b) Kobayashi, S.; Kitamura, T.; Taniguchi, H.; Schnabel, W. *Chem. Lett.* **1983**, 1117−1120.
(30) Sano, S.; Sano, T.; Morishima, I.; Shiro, Y.; Maeda, Y. *Proc. Natl. Acad. Sci. U.S.A.* **1986**, *83*, 531−535.
(31) Johnson, J. A.; Olmstead, M. M.; Stolzenberg, A. M.; Balch, A. L. *Inorg. Chem.* **2001**, *40*, 5585−5395.
(32) Bahrami, H.; Zahedi, M.; Safari, N. *J. Inorg. Biochem.* **2006**, *100*, 1449−1461.
(33) McDaniel, D. H.; Brown, H. C. *J. Org. Chem.* **1958**, *23*, 420−427.
(34) Kadish, K. M.; Morrison, M. M. *Bioinorg. Chem.* **1977**, *7*, 107−115.
(35) Quimby, D. J.; Longo, F. R. *J. Am. Chem. Soc.* **1975**, 5111−5117.
(36) Frisch, M. J.; Trucks, G. W.; Schlegel, H. B.; Scuseria, G. E.; Robb, M. A.; Cheeseman, J. R.; Scalmani, G.; Barone, V.; Mennucci, B.; Petersson, G. A.; Nakatsuji, H.; Caricato, M.; Li, X.; Hratchian, H. P.; Izmaylov, A. F.; Bloino, J.; Zheng, G.; Sonnenberg, J. L.; Hada, M.; Ehara, M.; Toyota, K.; Fukuda, R.; Hasegawa, J.; Ishida, M.; Nakajima, T.; Honda, Y.; Kitao, O.; Nakai, H.; Vreven, T.; Montgomery, J. A., Jr.; Peralta, J. E.; Ogliaro, F.; Bearpark, M.; Heyd, J. J.; Brothers, E.; Kudin, K. N.; Staroverov, V. N.; Kobayashi, R.; Normand, J.; Raghavachari, K.; Rendell, A.; Burant, J. C.; Iyengar, S. S.; Tomasi, J.; Cossi, M.; Rega, N.; Millam, J. M.; Klene, M.; Knox, J. E.; Cross, J. B.; Bakken, V.; Adamo, C.; Jaramillo, J.; Gomperts, R.; Stratmann, R. E.; Yazyev, O.; Austin, A. J.;Cammi, R.; Pomelli, C.; Ochterski, J. W.; Martin, R. L.; Morokuma, K.; Zakrzewski, V. G.; Voth, G. A.; Salvador, P.; Dannenberg, J. J.; Dapprich, S.; Daniels, A. D.; Farkas, O.; Foresman, J. B.; Ortiz, J. V.; Cioslowski, J.; Fox, D. J. Gaussian 09, Revision A.02; Gaussian, Inc.: Wallingford, CT, 2009.